The 2009 IEEE/RSJ International Conference on
Intelligent Robots and Systems
October 11-15, 2009 St. Louis, USA

# Insect-Like Mapless Navigation Based on Head Direction Cells and Contextual Learning Using Chemo-Visual Sensors

Zenon Mathews, Miguel Lechón, J.M. Blanco Calvo, Anant Dhir
Armin Duff, Sergi Bermúdez i Badia and Paul F.M.J. Verschure

*Abstract*— **We present a novel biomimetic approach to mapless autonomous navigation based on insect neuroethology. We implemented and tested a real-time neuronal model based on the Distributed Adaptive Control framework. The model unifies different aspects of insect navigation and foraging including landmark recognition, chemical search, path integration and optimal memory usage. Consistent with recent findings the model supports navigation using heading direction information, thus precluding the use of global information. We tested our model using a mobile robot performing a foraging task. While foraging for chemical sources in a wind tunnel, the robot memorizes the followed trajectories, using information from landmarks and heading direction accumulators. After foraging, landmark navigation is tested with the odor source turned off. Our results show stability against robot *kidnapping* and generalization of homing behavior to stable mapless landmark navigation. This demonstrates that allocentric and efficient goal-oriented navigation strategies can be generated by relying on purely local information.**

## I. INTRODUCTION

Navigation skills in unknown environments are essential for the survival of foraging animals. Foraging is a common feature carried out successfully by a wide range of animals, from mammals to insects [1], [2], [3], [4]. Some remarkable behaviors such as landmark navigation, homing, path integration (PI) and learning are in many occasions required to perform successful foraging.

The concept of *cognitive map* for navigation, carried out mainly by Tolman [5], was fuelled by the discovery of the so-called place cells in the hippocampus of the rat and has widely increased our understanding of cognitive navigation mechanisms [6], [7]. It spawned early research on navigational strategies in cognitive neuroscience based on hippocampal representations of space [8], [9], [10]. While mammals are assumed to learn a place/map-like representation for foraging [6], [7], this does not seem the case in insects.

Insect navigation has been studied for more than a century [11], [12], [2], [13]. Interestingly, a wide range of findings suggests that insects do not rely on a map for solving foraging tasks [14], [12]. Recent studies suggest that rather than using map-like representations, insects make optimal use of proprioception, landmark recognition and memory to navigate [4]. In particular, desert ants use sun position and visual panorama for heading direction computation [2], [15]. Complex allocentric navigational behaviors using mainly ego-centric cues can be seen both in mammals like rodents but also in insects like ants and bees, which have considerably lower computational resources with only hundreds of thousands of neurons. Therefore, insect navigation studies are useful in that they reveal essential components for an efficient mapless navigation strategy. This is especially relevant for robotic implementations of autonomous systems and artificial foragers.

Despite massive advances in computing power and classical branches of robotics [16], [17], [18], [19], robotic autonomous navigation, even with the use of global positioning information, remains a challenge. Until today a number of neurobiologically plausible models of navigation paradigms have been proposed for mobile robots [20], [21]. In the wake of neurobiological studies of place-cells, biomimetic robotic models of map-based navigation have recently seen great interest [21], [22], [23], [24]. The above mentioned models explain navigation from place to place only in very restricted familiar environments like mazes and small enclosures [25]. Navigators using such map based models of navigation are required to learn those place representations [26], [27]. Moreover, only a few of those models have been tested with real robots [22], [24]. As map based navigation strategies suffered from an inability to traverse unvisited regions of space, newer theories have incorporated path integration and head direction signals [28]. Even more recent versions also include cortical grid cells but still concentrate on the self-localization aspect of navigation rather than navigation between places [29], [30]. At the same time, the parsimonious navigation strategies of insects offer a guideline for computationally cheaper and eventually simpler navigation methods for mobile robots. A number of models exploit and reproduce some of the capabilities required during foraging [31], [32], [33]. However, many are biologically unrealistic and only deal with a very limited foraging task.

This paper describes a comprehensive mapless biologically based model, including chemical search, PI and landmark navigation, of insect navigation strategies that is implemented in the framework of the Distributed Adaptive Control (DAC) [34], [35]. The organization of behavior and optimal use of

The research leading to these results has received funding from the European Community's Seventh Framework Programme (FP7/2007-2013) under grant agreement no. 216916 for NEUROCHEM and EU SYNTHETIC FORAGER (FP7-217148) projects.

All authors are with the SPECS laboratory at Institut Universitari de l'Audiovisual (IUA) of the technology department of Universitat Pompeu Fabra (UPF) in Barcelona, Spain (telephone: +34 93 542 22 01, zenon.mathews@upf.edu

A.D. is also with Institute of Neuroinformatics at ETH and Uni Zürich, Switzerland

P.F.M.J.V. is also with Institució Catalana de Recerca i Estudis Avançats (ICREA) Barcelona, Spain.

landmark recognition, proprioceptive information, heading direction information and memory usage is controlled by DAC and tested on an artificial foraging ant robot. Our results show a successful integration of a number of biologically based models and behaviors that give rise to realistic foraging. Moreover, our model explains the generalization process as a probabilistic use of memory, which generates allothetic behavior from a limited set of idiothetic cues.

## II. METHODS

### A. Experimental setup

The experimental scenario consists of a robot forager called *SyntheticAnt*, which is tested in a controlled indoor environment (figure 1). The test environment consists of a wind tunnel used by *SyntheticAnt* to localize the feeder tracking an odor plume. The wind tunnel floor contains a set of visual cues (landmarks) for *SyntheticAnt* to learn its way through the environment. A vision based overhead tracking system (AnTS) is used to localize the robot and compute its heading direction within the test arena, allowing for an analysis of the behavior of the robot.

### B. Task

The task of the *SyntheticAnt* is to perform foraging using chemical sensing to localize food (odor source), and vision to learn to navigate through the environment, followed by successful homing. *SyntheticAnt* leaves its nest (marked by a unique visual cue) embarking on a foraging task to find a food source by following an odor plume up to its source (marked by another visual cue). On this outgoing route, the robot detects visual cues placed on the floor while performing foraging. Meanwhile collission avoidance has to be performed using proximity sensors. Upon feeder detection, it has to return to the nest using path integration information and restart foraging again. After foraging, landmark memorization is tested by placing the robot in an arbitrary location in the absence of the odor plume. Hence, in order to achieve this, *SyntheticAnt* has to recall the memorized landmarks and be able to navigate to other landmarks, including the nest and the feeder.

### C. Foraging Model

*SyntheticAnt* is based on the Distributed Adaptive Control (DAC) architecture [34], [36] for the integration of a number of biologically based models and behaviors that give rise to a realistic foraging behavior. DAC consists of three, tightly coupled, layers for behavioral control; the reactive, adaptive and contextual layers (figure3). The reactive control layer provides the behaving system with a pre-wired repertoire of reflexes such as collision avoidance, chemosearch, homing etc. The adaptive layer provides the mechanisms for the processing and classification of sensory events. The sensor and motor representations formed at the level of the adaptive layer provide the input to the contextual layer, which acquires, retains, and expresses sequential representations by means of short-term and long-term memories. These representations are used to plan ongoing behavior, and have

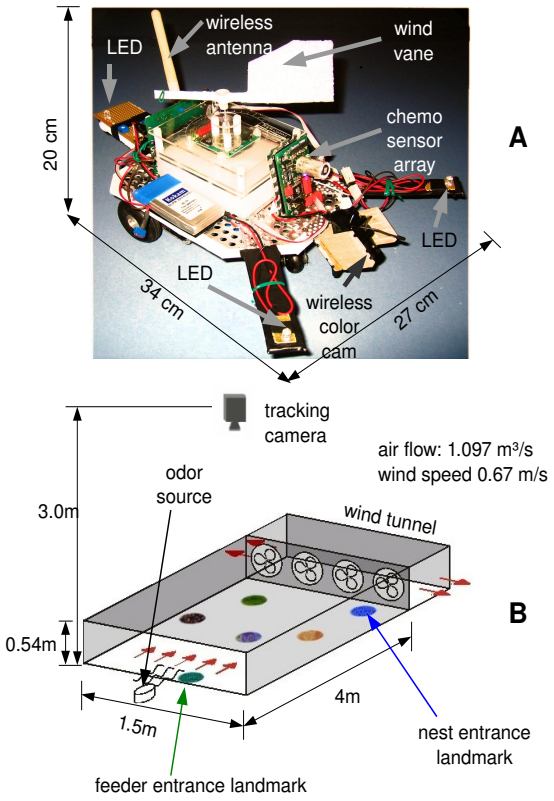


Fig. 1. **(A) The artificial forager *SyntheticAnt*.** The robot is equipped with a wireless color camera for visual cue recognition, a chemosensor array for odor detection, a wind sensor for wind direction computation and three LEDs for head direction computation using an overhead tracking system. The camera image is transmitted using a 2.4 GHz analogue wireless link. The exchange of motor commands and sensor readings with the robot are realized via a serial port over Bluetooth. **(B) Wind tunnel arena.** At the back of the wind tunnel there are exhaust ventilators that create a controlled wind flow inside the tunnel. Visual cues are placed on the floor and an overhead vision based tracking system (AnTS) is used to reconstruct the position and heading direction of the robot.

been shown to be compatible with formal Bayesian models of decision making [36]. All computations are implemented using the neural simulation tool IQR [37].

### D. Reactive behaviors

The reactive layer of *SyntheticAnt* implements a set of reactive behaviors including:

- *Chemical search: SyntheticAnt* implements a model based on the best studied case of chemotactic behavior, moth chemotaxis (as in [33]). It consists of an upwind movement (surge) whenever the animal perceives the odor stimulus and otherwise an oscillatory crosswind search (cast) until the odor plume is found again.
- *Collision avoidance:* Virtual proximity sensors, derived from the tracking system (figure 1), are used to avoid immediate collissions.
- *Feeder detection:* After finding the feeder (odor source) *SyntheticAnt* returns to the nest using a computed home vector by means of path integration, further referred to as

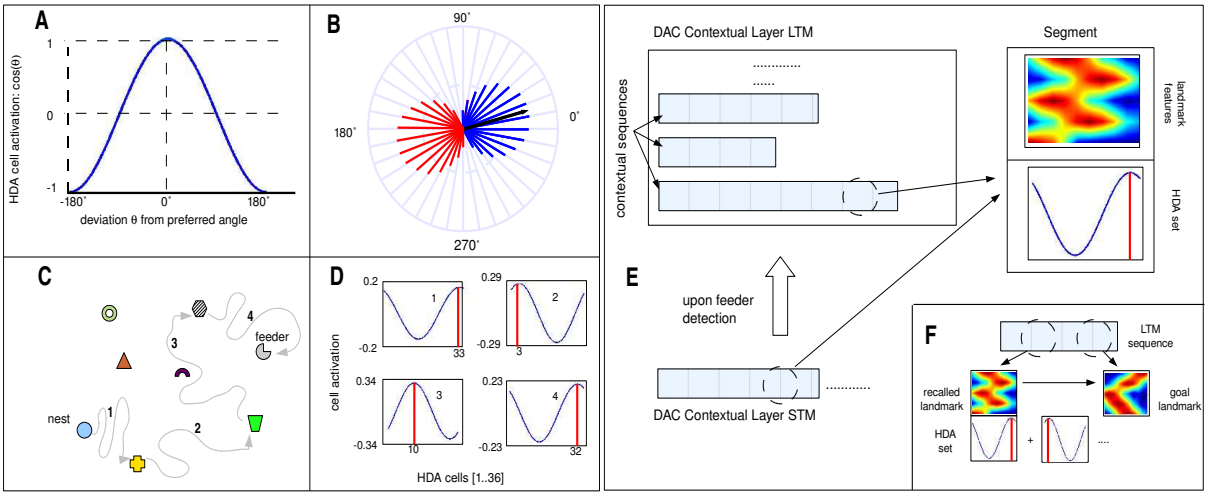


Fig. 2. **Contextual learning of landmarks:(A)** Activation of HDA cells as a sinusoidal function of the angular difference from the cell's preferred angle. **(B)** HDA-set activation for a group of 36 HDA cells (of 10° resolution each) for a movement indicated by the arrow. Blue and red lines represent positive and negative activations respectively. Each HD accumulator cell stores the value $d \times cos\theta$ where $d$ is the distance indicated by the movement arrow and $\theta$ the deviation angle of the movement from the preferred angle of the accumulator cell. The slope of activation falls as a sinusoidal function of angular deviation from the actuated direction, being 0 at 90°. **(C)** An example of a foraging run from nest to feeder traversing some landmarks indicated by the colored shapes. Individual path segments from landmark to landmark are indicated by numbers 1..4. **(D)** HDA cell activities at the end of each path segment. Y axis represents the cell activity and correlates with the distance traveled in the preferred angle of each cell, i.e. distance coded as firing rate. The X axis stands for the accumulator cells 1 to 36. The red vertical line with the corresponding number at the X axis shows the accumulator cell with the highest activity. **(E)** During the foraging runs from the nest to the feeder, the encountered landmarks are chained in the DAC contextual layer short-term memory (STM) together with the HDA set. Upon feeder detection, the contents of the STM are transferred into the LTM and the HDA-set is reset. After several foraging runs, the LTM contains several segment sequences of different lengths since in each foraging run only a subset of available landmarks are visited. **(F)** During the recall phase, the HDA-sets starting from the recalled segment to the goal segment are combined to compute the optimal route to the feeder. Note that the recalled segment and the goal segment can be on different LTM sequences, in which case the segments from the current landmark to the nest on one sequence, and the nest to the goal landmark on the other have to be combined.

*homing*.

In the absence of the odor plume *SyntheticAnt*'s surge-and-cast reactive behavior simplifies to a simple cast, which enables *SyntheticAnt* to explore the environment until a memorized landmark is encountered. In the absence of the odor plume a stochastic behavior is employed to avoid getting stuck.

### *E. Landmark Recognition*

Landmark recognition is implemented using a neural network that extracts prominent hue and edge features of visited landmarks using a neural network for extracting salient landmark features from the camera image using the neural simulation tool IQR [37]. See table I for the neural network parameters.

### *F. Heading Direction Accumulation*

Path integration (PI) uses self-motion cues to compute the vector between the navigator's current position and the starting point, i.e. home base. In our model we make use of heading direction and proprioceptive information to acquire PI. We propose the use of head direction accumulators (HDA), as postulated in [25]. A HDA is a neuron that fires only when the navigator heads in a particular direction. Furthermore, the firing rate of such a neuron correlates with the distance covered in that direction (figure 2, B). HDAs are assumed to integrate sensory information such as optic flow, polarized photoreceptors, sun position and proprioceptive information until reset [25]. Hence, a group of HDA neurons each of which is tuned to a different angle at equal intervals covering 0 to 360 degrees encodes the direction and distance from the previous position at which the HDA-set was reset. The activation of an HDA-set is governed by a cosine function as shown in figure 2. The slope of the activation rate is highest when the navigator moves in the HDA cell's preferred direction and falls according to the cosine function with angular deviation, consistent with [25] [38]. During foraging, whenever *SyntheticAnt* encounters a landmark, the set of detected landmark features and the current HDA information is passed to the STM of the contextual layer of DAC, as discussed in the next subsection. After that, the HDA-set is reset and the foraging continues.

### *G. Short and Long Term Memory*

The contextual layer supports the formation of more complex representations of perception and events (processed by the adaptive layer) expressing their relationship in time. In the case of the *SyntheticAnt*, pairs of visual cues and HDA information form basic memory elements, called memory segments. During the acquisition phase (foraging) salient events (cue detections) are first stored in short-term memory (STM) together with the current HDA. When the goal state

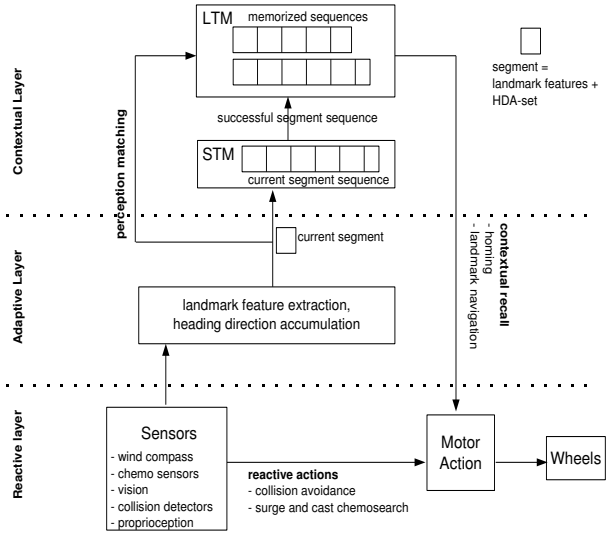


Fig. 3. ***SyntheticAnt*** **Foraging Model:** The reactive layer performs reflex actions like collision avoidance, chemical search, homing, etc. During foraging, the adaptive layer performs landmark recognition, feature extraction, HDA computation and constructs memory segments for each observed landmark. A segment, as shown on the top right, contains the extracted landmark features and an HDA-set. These segments are sequenced temporarily in the short-term memory (STM) of the contextual layer until feeder detection, when the contents of the STM are transferred into the long-term-memory (LTM). During the recall phase (homing, landmark navigation), the LTM is matched against the current sensory events and an optimal trajectory is computed from recalled LTM segments.

is reached, the content of the STM is stored in the long-term memory (LTM) as a sequence (figure 3). During the recall phase (landmark navigation), the LTM is matched against the current sensory events. Goal cue is defined as a the feature set characterizing a specific landmark. Matching LTM sequences containing both current sensory perception and goal cues are recalled to compute the optimal route from the current position to the goal landmark. Matching is accomplished by the following distance function:

$$d(a,b) = \frac{1}{K}\sum_i |\frac{a_i}{max(a)} - \frac{b_i}{max(b)}| \qquad (1)$$

where $a$ and $b$ are vectors in $\mathbb{R}^K$ and $a$ is the current activity of the cue information and $b$ is the stored cue information. A segment is selected when the distance $1 - d(a,b)$ is higher than a predefined threshold. The selected segment and segments stored in the same sequence together contain the accumulated PI information (HDA) to the goal.

To compute the optimal route from the currently perceived landmark to an arbitrary landmark, we consider the scenario where the currently selected segment (landmark) and the goal segment (landmark) are on different LTM sequences. To do this, we first compute the homing vector by summing and inverting the sequence of HDA-sets stored in all segments from the currently selected segment until nest on the first sequence. To this we add the sum of the HDA-s from nest to the goal segment (landmark) on the second sequence. This allows computing optimal routes between any two landmarks represented in arbitrary segments in the whole LTM.

After multiple foraging runs, *SyntheticAnt* might encounter landmarks, that had been seen in different foraging runs. This fact will select segments of different sequences in the LTM during recall. In this case, each selected segment will return a homing vector, which have to be merged optimally. This generalizes from homing to landmark navigation if the goal landmark is not the nest. In general we refer to the decoded heading direction and distance as *action* (or action HDA-set). Assuming a white noise error, this decoded heading direction and distance to the goal can be formulated as a 2D Gaussian probability distribution:

$$\bar{\boldsymbol{X}} \sim \boldsymbol{N}(\bar{\boldsymbol{\mu}}, \boldsymbol{\sigma^2}) \qquad (2)$$

where $\bar{X} = [\alpha, \delta]^T$. $\alpha$ is the angle and $\delta$ the distance coded by the action HDA-set. The action HDA-set, $\bar{X}$, can be formulated as a Gaussian distribution with mean $\bar{\mu}$ and variance $\sigma^2$. The variance $\boldsymbol{\sigma^2}$ grows with the total distance $dist$ covered during the heading direction accumulation. This can generally formulated as a function: $\sigma^2 = f(dist)$. Given this Gaussian distribution for each recalled segment action, we use Bayesian inference to compute the best action. If $n$ actions are recalled, the best action $a$ is the action with the highest conditional probability: $P(a|\bar{X}_1, \bar{X}_2, ..., \bar{X}_n)$. And using Bayes theorem., the probability of the optimal action is computed:

$$P(a|\bar{X}_1, \bar{X}_2, ..., \bar{X}_n) = \frac{P(a)P(\bar{X}_1, \bar{X}_2, ..., \bar{X}_n|a)}{P(\bar{X}_1, \bar{X}_2, ..., \bar{X}_n)} \qquad (3)$$

where the numerator $P(a)P(\bar{X}_1, \bar{X}_2, ..., \bar{X}_n|a)$ is the joint distribution $P(a, \bar{X}_1, \bar{X}_2, ..., \bar{X}_n)$ and the denominator $P(\bar{X}_1, \bar{X}_2, ..., \bar{X}_n)$ is a constant without effect.

Using conditional independence of memory sequences, the above equation can be reformulated as:

$$P(a|\bar{X}_1, \bar{X}_2, ..., \bar{X}_n) \propto P(a)\prod_i^n P(\bar{X}_i|a) \qquad (4)$$

$P(a)$ is uniformly distributed in an a priori unknown environment. Therefore, the computation of $P(a)$ in equation 4 can be reduced to the product of Gaussians $\bar{X}_1, \bar{X}_2, ..., \bar{X}_n$. The resulting action with the highest probability is optimal in the Bayesian sense.

*SyntheticAnt* runs on an Intel(R) Core(TM)2 Duo CPU 2.66GHz machine with GNU/Linux Suse10.3 operating system at about 35 Hz. The parameters of the neural simulation using the IQR toolkit [37] is summarized in table I.

## III. RESULTS

*SyntheticAnt* was exposed to a number of tests in the arena shown in figure 1, where it had to forage starting from the nest and to find the feeder placed at the upwind end of the wind tunnel. Upon feeder detection it had to compute the homing vector and return to nest. After foraging runs, the chemical cue was switched off and *SyntheticAnt* was kidnapped and placed in an arbitrary position in the arena.

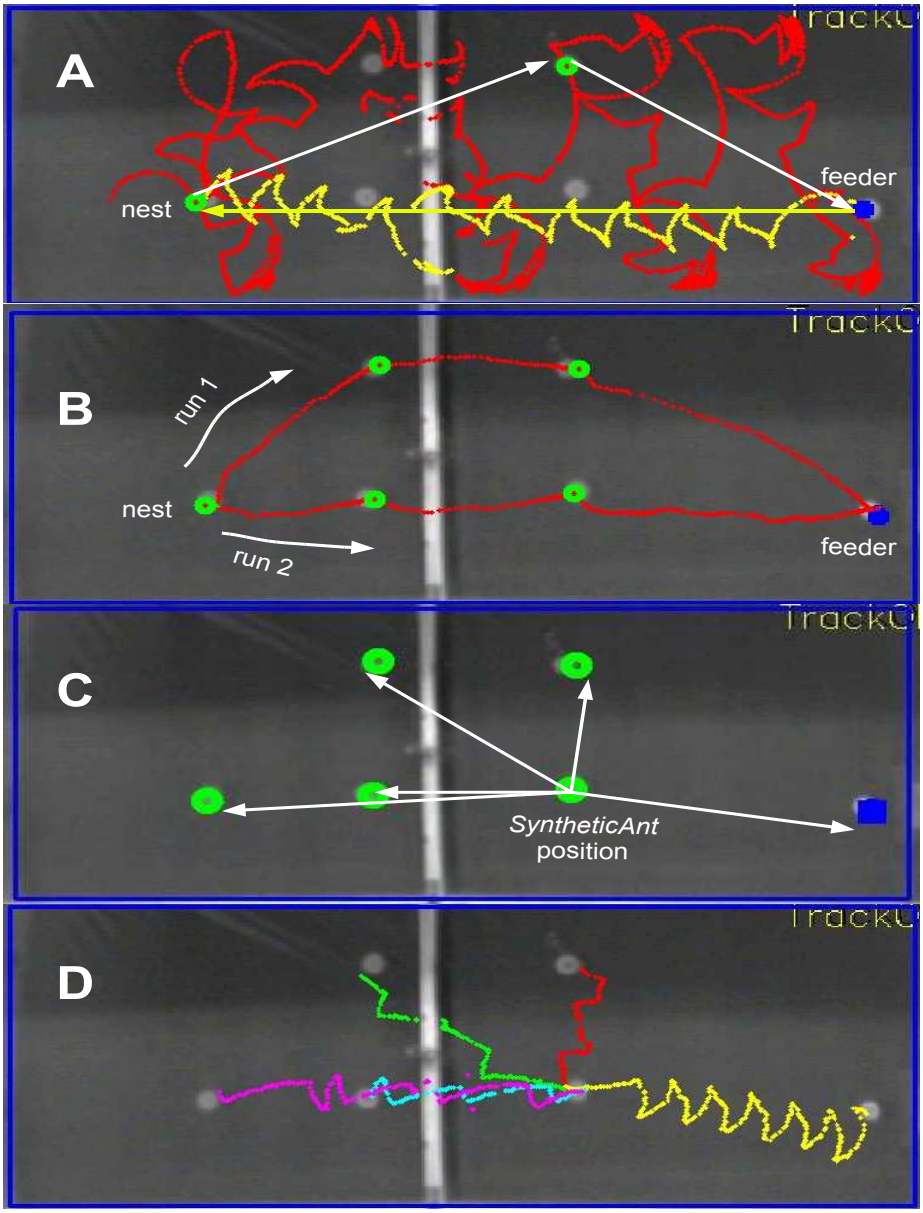


Fig. 4. **Foraging, homing and landmark navigation:** All plots are superimposed on the image from the tracking camera. The vertical bar in the middle of the image belongs to the wooden structure of the wind tunnel and does not interfere with the movement freedom of *SyntheticAnt*. **(A) Foraging and homing.** The red dots indicate position of *SyntheticAnt* during chemosearch (foraging) from nest to feeder. The upwind anemotactic chemosearch using the surge-and-cast algorithm gives rise to the oscillatory movement until the odor plume can be sensed. The green circles indicate encountered landmarks. Note that not all available landmarks are detected. The white arrows indicate the corresponding HDA sets memorized using the DAC contextual layer. The blue square on the right is the feeder. The yellow arrow corresponds to the computed homing HDA. The yellow track shows the homing behavior of the robot after feeder detection. The homing path shows a zig-zag movement as the robot tries to correct its current heading direction using the difference between the accumulated HDA starting at the feeder and the contextual memory response HDA. Such a correction is equivalent of the general proportional controller. **(B) Different nest to feeder trajectories.** To test the generalization of homing to landmark navigation, we forced *SyntheticAnt* to go on two different trajectories from nest to feeder (indicated as run 1 and run 2, leading through available landmarks. During these runs encountered landmarks (shown in green) and the corresponding HDA sets are memorized. Note that all available landmarks are detected in both the runs together, in order to test the recall. **(C) Kidnapping and generalization of homing.** After the runs shown in B, *SyntheticAnt* is kidnapped and placed in an arbitrary position in the arena. *SyntheticAnt* employs the cast behavior (not shown in figure) until it finds a landmark it had memorized (shown as the *SyntheticAnt* position). Thereafter it recalls all possible straight routes to other landmarks including the nest and feeder, indicated by the white arrows. **(D) Navigation of recalled routes.** After recalling routes to other landmarks as shown in C, *SyntheticAnt* carries out the traversal of the recalled route until the goal landmark is recognized. The different trajectories are plotted in different colors.

| | |
|---|---|
| # total neurons | 62771 |
| # total neuron groups | 252 |
| # integrate and fire | 29 |
| # linear threshold | 202 |
| # random spike | 21 |
| # total synapses | 103872 |
| # cells in HDA set | 72 |
| # cells in landmark features | $2 \times 4$ |
| processes | 16 |

TABLE I

NEURAL SIMULATION PARAMETERS

At this point, it had to find a landmark and reach other landmarks and the feeder by generating optimal routes.
An overhead camera is used to track the position of the robot for data analysis, together with the logged data from the neural simulation of the model. Figure 4 A, shows a foraging run through landmarks and homing behavior on a straight line to the nest from the feeder. Encountered landmarks during the foraging run are shown as green circles in figure 4, A. The nest is indicated by the blue rectangle. After a foraging run, when the feeder is found, the homing vector is recalled automatically and the DAC reactive layer of *SyntheticAnt* initiates the homing behavior. *SyntheticAnt* is also able to generalize homing to landmark navigation and can traverse unknown paths to go from a given landmark to another landmark encountered during a different foraging run (figure 4 B,C,D)[1].

Memorized and computed HDA sets are direction vectors leading from one landmark to another (shown as arrows in figure 4). Decoding of an HDA neuron group into the direction $\alpha$ is done as following:

$$\alpha = \frac{360}{N} * I$$

where $N$ is the number of neurons in the HDA set and $I$ the index of the neuron with highest activity in the set. The distance $D$ is coded directly by the activity rate of the neuron $I$. See also figure 2 A,B,C,D for HDA coding.

Figure 5 is the density plot of tracking data and summarizes the typical behavior of *SyntheticAnt* during 5 foraging runs. The landmark regions get very high density as landmark recognition stops the robot for some time to ensure precise feature extraction of the landmark. The robot stops to avoid collisions when at the periphery of the field and this results in some high density spots along the periphery.

The use of overhead tracking for the computation of the heading direction and proprioception of the *SyntheticAnt* gives highly precise HDA-sets. This is very useful for testing the feasibility of our insect model and also to conduct tests inside a wind tunnel. However, in real world experiments these computations will be erroneous due to sensor errors. Therefore in future work the overhead tracking will be replaced by odometry sensors (e.g. using optic flow) and heading direction sensors (e.g. using solar compass). This means that the precision of HDA computation will fall since such sensors have intrinsic errors. While error in heading direction and path integration accumulates with the distance traveled, the precision of the computed HDA falls. To evaluate the performance of our system when using such imperfect information, we conducted the following experiment. From three foraging runs of *SyntheticAnt* going through different landmarks, we evaluated the error in the computation of the homing vector when using one, two or three recalled DAC LTM sequences. Noise in the HDA sets for each path-segment in each sequence (from one landmark to the next), was modeled as linearly correlated with the distance traveled. Specifically a white noise of mean zero and a variable variance (SNR) proportional to the distance traveled was induced on each HDA set. After this, the homing vector was computed in three different ways: using each of the three sequences individually, by combining just two of the three and by combining all three together. The fusion of different sequences was done using the DAC Bayesian fusion algorithm described earlier (equation 4). We assessed the robustness of the system by measuring the error when varying the signal to noise ratio (SNR) from 0.1 to 100. Results show that the error falls with the number of sequences used to compute the homing vector (number of runs/experience of the forager) for all ranges of the SNR values of sensors, see figure 6. This not only justifies the Bayesian merging of LTM responses but also, it indicates the validity of the proposed insect-model also when using real odometry and heading direction sensors.

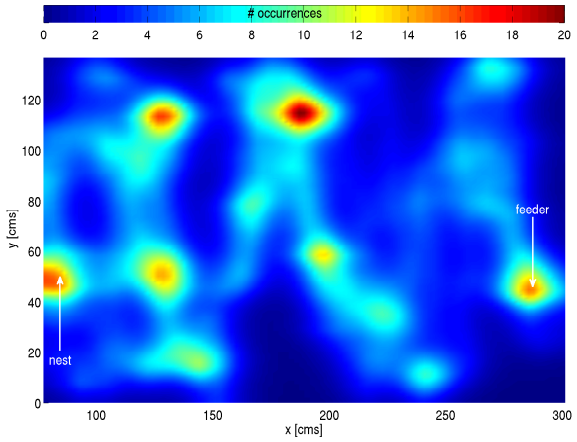


Fig. 5. **Foraging behavior as density plot:** Position data from five foraging runs of *SyntheticAnt* were used. The high density areas are near landmarks, the nest (leftmost high density circle) and feeder (rightmost high density circle). Also some peripheral areas have relatively high densities due to the fact that *SyntheticAnt* stops to avoid collisions. The plot illustrates the typical behavior of the robot during foraging. Note that the colorbar indicates the number of occurrences of the robot at a given position and a numerical interpolation was applied to smoothen the tracked position data.

A remarkable property of the three coupled control layers of DAC is the emergence of useful behavioral properties.

[1]A video clip provided in the supplementary material demonstrates the behavior of the robot during a foraging run.

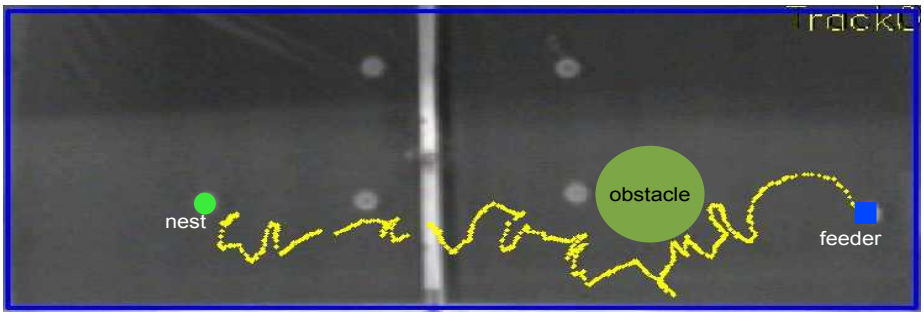


Fig. 7. **Acting in a dynamic world:** *SyntheticAnt* was exposed to obstacles placed on its route during homing or landmark navigation. In a typical example as in the figure, the collision avoidance reactive control competes with homing behavior and maneuvers *SyntheticAnt* around the collision. The heading direction to the nest is simultaneously corrected and the robot returns to nest. This capability emerges intrinsically from the three coupled layers of DAC and allows *SyntheticAnt* to act in a dynamically changing world with moving objects.

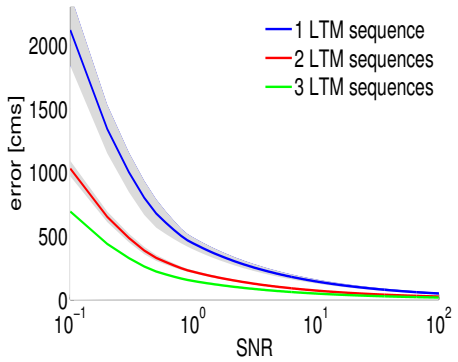


Fig. 6. **Bayesian merging of LTM sequences:** The error in homing vector computation (or in landmark to landmark route recall in general) is negatively correlated with the SNR of the HDA computation. For low SNRs (i.e. low precision sensors) the error rises drastically. Whereas for high SNRs (high precision sensors) it falls. The errors when using one, two or three LTM sequences in combination are plotted. The colored lines are mean values and the patches signify standard deviation. Using more LTM sequences is clearly preferable thanks to the Bayesian merging algorithm. The error falls for increasing number of LTM sequences used for all ranges of SNR values of sensors.

One of them is maneuvering in a dynamically changing world. To test this behavior we placed obstacles in the arena as *SyntheticAnt* was performing landmark navigation or homing. The collision avoidance reactive behavior then had to compete with the previously active behavior mode (e.g. homing or surge-and-cast) to maneuver around the obstacle. Thereby the desired heading direction has to be corrected for the movement of the robot. A typical example of such a maneuver is shown in figure 7.

## IV. CONCLUSIONS

We presented a mapless navigational model based on insect navigation strategies. This biologically based model includes different aspects of insect-navigation like chemical search, PI and landmark navigation and it is implemented using the Distributed Adaptive Control framework. Our model is implemented and tested on a ground robot in a chemo-foraging task. Unlike navigational models based on place/map like representations, our model uses heading direction accumulation and proprioceptive information in combination with landmark recognition. This approach proposes a solution to autonomous navigation without having the need to learn place representations. *SyntheticAnt* is able to learn a graph structure using local cues, heading direction accumulation and low memory usage. Consistent with insect studies, our model is stable against landmark addition or removal as this does not affect the learned DAC LTM. An interesting addition to the model would be *forgetting*, which would allow the forager to forget LTM sequences that include landmarks that were displaced after learning. Going beyond the insect world, the theory is also consistent with environmental exploration of rats, which move along wall edges and between prominent landmarks when placed in novel enclosures [14]. Such an exploration pattern was also observed in humans and is optimal for creating waypoints and heading vectors, but not optimal for creating a representation of continuous space [39]. Finally, as discussed in [25], the heading-vector framework unifies various navigation forms from rodents in laboratory environments to long distance bird migration. Taking parsimony as the principle behind optimality, insect navigation strategies as the one proposed in this model provide inspiration for future work on mobile robots that act in the real-world. DAC thereby provides the unifying framework for combining different aspects of perception, memory and behavior.

## V. ACKNOWLEDGMENTS

The research leading to these results has received funding from the European Community's Seventh Framework Programme (FP7/2007-2013) grant agreement no. 216916 for the NEUROCHEM and from the (FP7-217148) SYNTHETIC FORAGER projects. The authors would like to thank Hector Tapia Simó for help in maintaining the *SyntheticAnt* and Eduard Sellabona for editing the foraging video clip.

## REFERENCES

[1] D. Stephens, J. Brown, and R. Ydenberg, *Foraging:Behavior and Ecology*. Chicago: University of Chicago Press, 2007.

[2] R. Wehner, "Desert ant navigation: how miniature brains solve complex tasks," *Journal of comparative physiology.A, Neuroethology, sensory, neural, and behavioral physiology*, vol. 189, no. 8, pp. 579–588, Aug 2003.

[3] H. Wolf and R. Wehner, "Pinpointing food sources: olfactory and anemotactic orientation in desert ants, Cataglyphis fortis," *J Exp Biol*, vol. 203, no. 5, pp. 857–868, 2000.

[4] T. S. Collett and M. Collett, "Memory use in insect visual navigation," *Nature reviews.Neuroscience*, vol. 3, no. 7, pp. 542–552, Jul 2002.

[5] E. C. Tolman, "Cognitive maps in rats and men." *Psychological review*, vol. 55, no. 4, pp. 189–208, July 1948.

[6] J. O'Keefe and J. Dostrovsky, "The hippocampus as a spatial map. preliminary evidence from unit activity in the freely-moving rat," *Brain research*, vol. 34, no. 1, pp. 171–175, Nov 1971.

[7] J. O'Keefe and L. Nadel, *The Hippocampus as a Cognitive Map*. Oxford University Press, USA, 1978-12-07 1978.

[8] J. O'Keefe, *The hippocampal cognitive map and navigational strategies*. Oxford University Press, USA, 1991.

[9] M. A. Brown and P. E. Sharp, "Simulation of spatial learning in the morris water maze by a neural network model of the hippocampal formation and nucleus accumbens," *Hippocampus*, vol. 5, no. 3, pp. 171–188, 1995.

[10] R. U. Muller, M. Stead, and J. Pach, "The hippocampus as a cognitive graph," *The Journal of general physiology*, vol. 107, no. 6, pp. 663–694, Jun 1996.

[11] K. von Frisch, "Decoding the language of the bee," *Science (New York, N.Y.)*, vol. 185, no. 4152, pp. 663–668, Aug 23 1974.

[12] T. S. Collett, "Insect navigation: visual panoramas and the sky compass," *Current biology : CB*, vol. 18, no. 22, pp. R1058–61, Nov 25 2008.

[13] A. Si, M. V. Srinivasan, and S. Zhang, "Honeybee navigation: properties of the visually driven 'odometer'," *The Journal of Experimental Biology*, vol. 206, no. Pt 8, pp. 1265–1273, 2003.

[14] R. Wehner, M. Boyer, F. Loertscher, S. Sommer, and U. Menzi, "Ant navigation: one-way routes rather than maps," *Current biology : CB*, vol. 16, no. 1, pp. 75–79, Jan 10 2006.

[15] S. Akesson and R. Wehner, "Visual navigation in desert ants cataglyphis fortis: are snapshots coupled to a celestial system of reference?" *The Journal of experimental biology*, vol. 205, no. Pt 14, pp. 1971–1978, Jul 2002.

[16] R. Benenson, S. Petti, T. Fraichard, and M. Parent, "Towards urban driverless vehicles," *International Journal of Vehicle Autonomous Systems*, vol. 6, no. 1/2, pp. 4–23, 2006.

[17] H. Andreasson, A. Treptow, and T. Duckett, "Localization for mobile robots using panoramic vision, local features and particle filter," *Robotics and Automation, 2005. ICRA 2005. Proceedings of the 2005 IEEE International Conference on*, pp. 3348–3353, April 2005.

[18] E. Royer, J. Bom, M. Dhome, B. Thuilot, M. Lhuillier, and F. Marmoiton, "Outdoor autonomous navigation using monocular vision," *Intelligent Robots and Systems, 2005. (IROS 2005). 2005 IEEE/RSJ International Conference on*, pp. 1253–1258, Aug. 2005.

[19] A. J. Davison and N. Kita, "Sequential localisation and map-building for real-time computer vision and robotics," *Robotics and Autonomous Systems*, vol. 36, no. 4, pp. 171 – 183, 2001.

[20] M. O. Franz and H. A. Mallot, "Biomimetic robot navigation," *Robotics and autonomous Systems*, vol. 30, pp. 133–153, 2000.

[21] A. Arleo and W. Gerstner, "Spatial cognition and neuro-mimetic navigation: a model of hippocampal place cell activity," *Biological Cybernetics*, vol. 83, no. 3, pp. 287–299, 2000, article.

[22] C. Giovannangeli, P. Gaussier, and J.-P. Banquet, "Robustness of visual place cells in dynamic indoor and outdoor environment," *International Journal of Advanced Robotic Systems*, vol. 3, no. 2, pp. 115–124, jun 2006.

[23] C. Giovannangeli, P. Gaussier, and G. Desilles, "Robust mapless outdoor vision-based navigation," *Intelligent Robots and Systems, 2006 IEEE/RSJ International Conference on*, pp. 3293–3300, Oct. 2006.

[24] C. Giovannangeli and P. Gaussier, "Autonomous vision-based navigation: Goal-oriented action planning by transient states prediction, cognitive map building, and sensory-motor learning," *Intelligent Robots and Systems, 2008. IROS 2008. IEEE/RSJ International Conference on*, pp. 676–683, Sept. 2008.

[25] J. L. Kubie and A. A. Fenton, "Heading-vector navigation based on head-direction cells and path integration," *Hippocampus*, Dec 12 2008.

[26] A. Guanella and P. F. M. J. Verschure, "Prediction of the position of an animal based on populations of grid and place cells: a comparative simulation study," *Journal of Integrative Neuroscience*, vol. 6, pp. 433 – 446, 2007.

[27] R. Wyss and P. F. M. J. Verschure, "Bounded invariance and the formation of place fields." *Advances in Neural Information Processing Systems NIPS*, 2003.

[28] D. S. Touretzky and A. D. Redish, "Theory of rodent navigation based on interacting representations of space," *Hippocampus*, vol. 6, no. 3, pp. 247–270, 1996.

[29] M. E. Hasselmo and M. P. Brandon, "Linking cellular mechanisms to behavior: entorhinal persistent spiking and membrane potential oscillations may underlie path integration, grid cell firing, and episodic memory," *Neural plasticity*, vol. 2008, p. 658323, 2008.

[30] B. L. McNaughton, F. P. Battaglia, O. Jensen, E. I. Moser, and M. B. Moser, "Path integration and the neural basis of the 'cognitive map'," *Nature reviews.Neuroscience*, vol. 7, no. 8, pp. 663–678, Aug 2006.

[31] S. Bermudez i Badia, P. Pyk, and P. F. M. J. Verschure, "A fly-locust based neuronal control system applied to an unmanned aerial vehicle: the invertebrate neuronal principles for course stabilization, altitude control and collision avoidance," *The International Journal of Robotics Research*, vol. 26, p. 759, 2007.

[32] U. Bernardet, S. Bermudez i Badia, and P. F. M. J. Verschure, "A model for the neuronal substrate of dead reckoning and memory in arthropods: a comparative computational and behavioral study," *Theory in Biosciences*, vol. 127, pp. 163 – 175, 2008.

[33] P. Pyk, S. B. i Badia, U. Bernardet, P. Knüsel, M. Carlsson, J. Gu, E. Chanie, B. S. Hansson, T. C. Pearce, and P. F. M. J. Verschure, "An artificial moth: Chemical source localization using a robot based neuronal model of moth optomotor anemotactic search," *Autonomous Robots*, vol. 20, no. 3, pp. 197–213, 2006.

[34] P. F. Verschure, T. Voegtlin, and R. J. Douglas, "Environmentally mediated synergy between perception and behaviour in mobile robots," *Nature*, vol. 425, no. 6958, pp. 620–624, Oct 9 2003.

[35] P. F. M. J. Verschure and P. Althaus, "A real-world rational agent: unifying old and new ai," *Cognitive Science A Multidisciplinary Journal*, vol. 27, no. 4, pp. 561–590, 2003.

[36] ——, "A real-world rational agent: Unifying old and new ai," *Cognitive Science*, vol. 27, pp. 561–590, 2003.

[37] U. Bernardet, M. Blanchard, and P. F. M. J. Verschure, "Iqr: a distributed system for real-time real-world neuronal simulation," *Neurocomputing*, vol. 44-46, pp. 1043–1048, 2002.

[38] R. W. Stackman and J. S. Taube, "Firing properties of rat lateral mammillary single units: head direction, head pitch, and angular head velocity," *The Journal of neuroscience : the official journal of the Society for Neuroscience*, vol. 18, no. 21, pp. 9020–9037, Nov 1 1998.

[39] H. J. Spiers and E. A. Maguire, "A navigational guidance system in the human brain," *Hippocampus*, vol. 17, no. 8, pp. 618–626, 2007.